ANALYSIS OF MULTI-PHASE LLC RESONANT CONVERTERS

E. Orietti[*], P. Mattavelli[**], G. Spiazzi[*], C. Adragna[***], G. Gattavari[***]

[*]Dept. of Information Engineering – University of Padova
Via Gradenigo 6/b, 35131 Padova, Italy. Tel.: +39.049.827.7755, Fax.: +39.049.827.7699
[**] Dept. of Technology and Management of Industrial Systems – University of Padova
Stradella S. Nicola 3, 36100 Vicenza, Italy. Tel.: +39.0444.998734
[***]ST Microelectronics, via C. Olivetti, 20041 Agrate Brianza (MI), Italy

***Abstract* - In this paper a topology for multi-phase interleaved LLC resonant converter is presented. The proposed solution, based on three LLC modules with transformer primary windings star connection allows to drastically reduce the output current ripple and consequently to minimize the output filter capacitor size. Differently from other multi-phase solutions, that are greatly susceptible to resonant component mismatch and consequently can be affected by a considerable current imbalance among modules, the proposed topology exhibits an inherent balancing capability. Small-signal analysis is presented and the possibility to turn-off one or two modules (phase shedding) at reduced output current levels is discussed, highlighting the trade-off between converter efficiency and output capacitor current ripple reduction. Measurements on a prototype will be included in the paper as validation of assertions and proposals.**

***Keywords* – LLC resonant converter, multi-phase interleaved converters.**

I. INTRODUCTION

Resonant converters have been confined in the last thirty years to niche applications such as very high-voltage applications or high fidelity audio systems while much effort was spent in research by industries and universities because of its attractive features: smooth waveforms, high efficiency and high power density. In recent times the LLC resonant converter [1,2], in particular in its half-bridge implementation, has been widely and successfully applied to flat panel TV, 80+ ATX and small form factor PC, where the requirements on efficiency, power density and EMC compliance of their switching mode power supplies (SMPS) are getting more and more stringent. However future SMPS requirements will have to face one of the few remaining drawbacks of LLC resonant converter topology that is related to the output filter capacitors volume that represents the major limit for such applications. The injection of rectified sine wave currents into the output filter capacitor can be adequately mitigated by the parallel use of multiple modules such as in interleaved buck solutions for voltage regulator modules. This topology has been presented in [3,4] for two modules operating with 90 degrees phase shift. One of the drawbacks of this solution is represented by the inherent current unbalance caused by resonant component mismatch that may cause one of the two modules to reduce its output power down to zero, thus requiring mandatory workarounds to overcome the problem [5].

In this paper a three-phase topology of LLC resonant converter will be presented to avoid this great drawback by means of three modules properly connected. The basic scheme of one LLC module and the main specifications for the proposed multiphase resonant converter are illustrated in Section II. In Section III the three-phase LLC converter will be introduced, highlighting the benefit in terms of output filter current ripple reduction. The effect of resonant component mismatch will also be explored and a suitable star connection solution will be investigated to overcome current derating limits by means of intrinsic balancing. Section IV will investigate the feasibility of phase-shedding for the three phase LLC resonant converter with star connection exploring the benefits in terms of converter efficiency, effects on current ripple reduction and switching frequency design. Measurements on a prototype will be included in the paper as validation of assertions and proposals.

II. LLC RESONANT CONVERTER PROTOTYPE

In this section the prototype of LLC resonant converter, with half-bridge topology, will be briefly introduced. The design of the power section of such converter is not the aim of the paper and more details can be found in literature [2,6-8]. The basic scheme of the prototype is depicted in Figure 1 and specifications listed in Table 1. As can be seen from the specifications, the LLC converter is intended to operate in conjunction with a boost PFC stage that regulates the resonant converter input voltage at 400V nominal. The isolation transformer uses the magnetic integration approach, incorporating the resonant series (L_R) and shunt (L_M) inductances. Thus, no additional external coils are needed for the resonance inductance. The transformer configuration chosen for the secondary windings is center-tap, and the output rectifiers are Schottky type diodes, in order to limit power losses. The output capacitor size is chosen quite large to conveniently reduce the output voltage ripple. The rectified "sine wave" output current presents indeed a large peak to peak ripple. Three identical modules were manufactured to fulfill the research purposes of this paper.

III. INTERLEAVED THREE PHASE LLC RESONANT CONVERTER

LLC resonant converters exhibit a large voltage ripple on output filter capacitor because of the rectified sine-wave current injected through the transformer secondary windings. In order to reduce the capacitor size and/or the steady-state output voltage ripple, the interleaved approach can be

profitably applied. In Figure 2 a multi-phase LLC resonant converter is depicted: three identical modules (specifications listed in Table 1) are parallel connected and switched at the same frequency but with 120 degrees phase-shift of their driving signals.

Figure 3 shows the benefit of an increasing number of parallel modules on the total rectified current ripple, that is the peak-to-peak AC current injected into the output filter capacitor. The results in Figure 3 are obtained from MATLAB Simulink simulations with 400 V input voltage, 24 V output voltage and different output currents. The huge reduction of total current ripple in the three modules solution can be appreciated as compared to one and two modules counterparts, suggesting the possibility to drastically reduce the output filter capacitor size.

The use of parallel connected LLC resonant converters to supply the same load and share the same output filter capacitor presents limitations and drawbacks caused by resonant devices mismatch. The modules are operated at the same switching frequency controlled by the voltage regulation loop, while resonant component mismatch causes the three phases to exhibit different voltage conversion ratios. As a consequence, the load current is no longer equally supplied by the modules and one of the phases may totally reduce its output power to zero. Table 2 illustrates the results of some measurements on the prototype for different operating conditions in presence of resonant device mismatch. In order to emphasize the mismatch the third module resonant capacitor has been increased by 12 % by adding a 2.7 nF capacitor in parallel to the nominal one (22 nF). It can be noticed from the data in the left-half of the table, that the third module delivers zero output current, in presence of resonant component mismatch. This condition is confirmed by the inspection of the primary-side currents shown in Figure 4(a) (400 V input voltage, 8 A output current condition): the primary-side current of the third module is indeed interested only by the magnetizing current.

In order to overcome such limitation, that is unavoidable in mass production, a three-phase topology is proposed, as depicted in Figure 5, where the transformers primary windings are star connected. This modification allows, by means of the voltage modulation of star connection point, to greatly reduce the mean current unbalance caused by component mismatch. From data shown in the right-half of Table 2, the intrinsic balancing capability of this topology is pointed out compared to the simple parallel connection. Moreover, the waveforms depicted in Figure 4(b) confirm the great balancing ability of the star connection topology compared to a simple parallel interleaved connection.

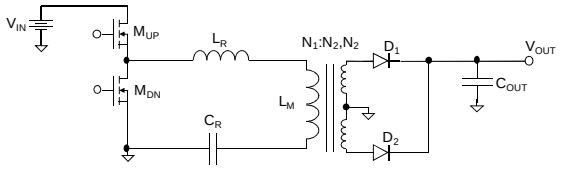

Fig. 1. Scheme of a single module LLC resonant converter.

TABLE 1
Specifications and component sizing for the LLC resonant converter.

V_{IN}	320-420	V
$V_{IN\text{-}NOMINAL}$	400	V
V_{OUT}	24	V
I_{OUT}	0-6	A
C_R	22	nF
L_R	110	µH
L_M	585	µH
C_{OUT}	(4400+470)	µF
N_1	36	Turns
N_2	4	Turns

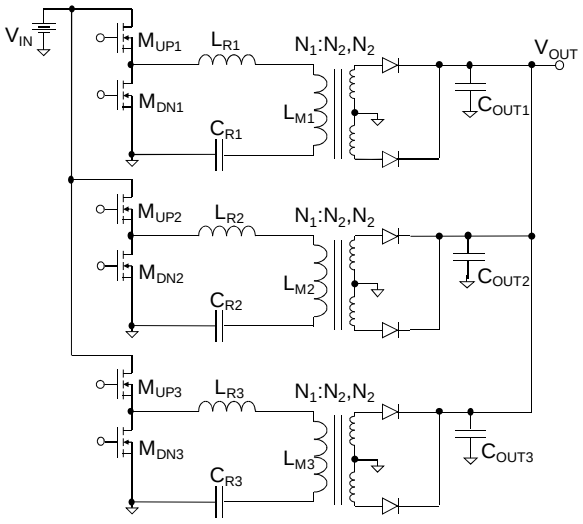

Fig. 2. LLC converter with three modules parallel connected.

TABLE 2
Average currents supplied by each module at different operating conditions (C_{R3} = C_R + 2.7 nF).

	SIMPLE PARALLEL CONNECTION (Figure 2)				STAR CONNECTION (Figure 3)			
	V_{IN} =320 V I_{OUT} = 6 A	V_{IN} =320 V I_{OUT} = 8 A	V_{IN} =400 V I_{OUT} = 6 A	V_{IN} =400 V I_{OUT} = 8 A	V_{IN} =320 V I_{OUT} = 6 A	V_{IN} =320 V I_{OUT} = 8 A	V_{IN} =400 V I_{OUT} = 6 A	V_{IN} =400 V I_{OUT} = 8 A
$I_{OUT\text{-}1}$ [A]	4.2	5.2	4.1	5.2	2.1	2.8	2.1	2.8
$I_{OUT\text{-}2}$ [A]	1.8	2.8	1.7	2.6	2.0	2.7	2.0	2.6
$I_{OUT\text{-}3}$ [A]	0	0	0.2	0.2	1.9	2.5	1.9	2.6

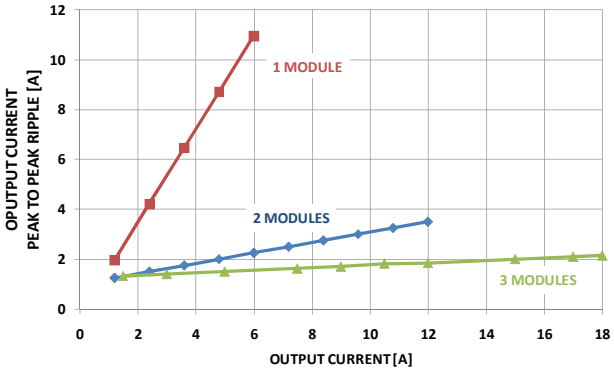

Fig. 3. Simulated peak to peak current injected on output filter capacitor as a function of output current: one module, two modules with 90° phase-shift and three modules with 120° phase shift. (@ V_{IN} = 400V)

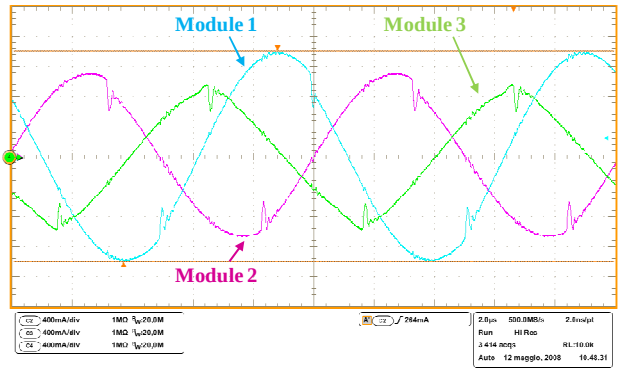

(a)

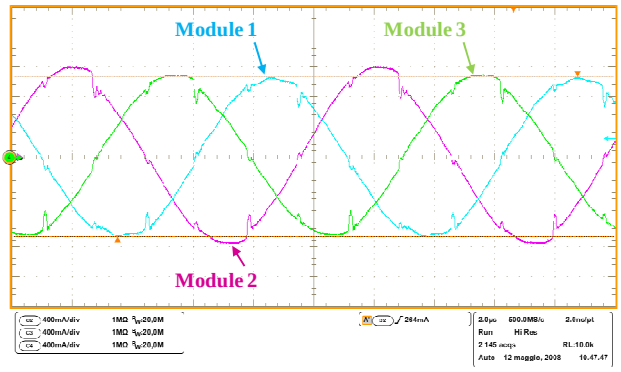

(b)

Fig. 4. Resonant currents flowing in the three modules of LLC converter (400 mA/div, 2 µs/div) with simple parallel connection (a) and with star connection of transformer primary windings (b) @ V_{IN} = 400 V, I_{OUT} = 8 A (C_{R3} = C_R + 2.7 nF)

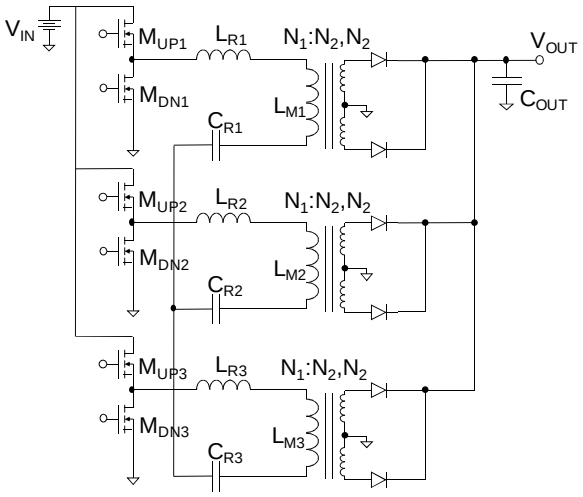

Fig. 5. Interleaved three phases LLC resonant converter using transformers primary windings star connection.

A. Voltage loop control design

The regulation of output voltage in a three-phase LLC resonant converter with star connection is performed as for other resonant converters by means of switching frequency modulation. To correctly design such voltage loop control, the small signal transfer function for the interleaved tree-phase converter should be determined and quantified. Generally speaking, the generalized state-space averaging method [9], that can be used to determine the transfer function of a single LLC converter, cannot be easily extended to the three-phase interleaved solution being the number of variables too wide for an analytical solving.

To overcome such limitation a simulation method can be adopted. The Bode diagram of the LLC small-signal transfer function ($\delta V_{OUT}/\delta T_{SW}$) from converter switching period (T_{SW}) to output voltage (V_{OUT}) can be evaluated through a series of simulations with different noise frequency values. The LLC model is operated open-loop, or with a very slow voltage control loop, at the desired operating point, while a small amplitude sinusoidal noise is superimposed to the switching period. That sinusoidal noise amplitude represents the δT_{SW} term and it is kept constant for all performed simulations, while its frequency/period is changed over the desired range for Bode diagram.

Generally, Bode diagrams from the converter switching period to output voltage ($\delta V_{OUT}/\delta T_{SW}$) can be easily transformed to the transfer function from converter switching frequency ($\delta V_{OUT}/\delta F_{SW}$) taking into account expression (1)

$$\delta F_{SW} \cong \delta T_{SW} \cdot F_{sw-nom}^2 \qquad (1)$$

where δT_{SW} represents the converter switching period perturbation caused by the sinusoidal noise, $F_{sw\text{-}nom}$ is the mean switching frequency without superimposed perturbations and δF_{SW} is the equivalent converter switching frequency perturbation. In the cases studied in the following,

the transfer functions exhibit a 197 dB constant gain shift of magnitude diagrams related to $F_{sw\text{-}nom}$ = 88.7 kHz.

The obtained simulation results, can be compared to the analytical Bode Diagram derived using the generalized state-space averaging method. Figure 6 depicts this comparison, for a 400 V input voltage, 6 A output current condition, suggesting the excellent agreement between simulations and mathematical calculation and therefore the possibility to use them without distinction. Bode diagrams depicted in Figure 6 represents the transfer function between the converter switching frequency and the output voltage.

Using the same simulation approach, the three-phase LLC converter with star connection transfer function was obtained for different operating points. It is interesting to notice that such transfer functions look pretty similar to the ones for a single module LLC converter, taking into account the 197dB gain shift between them. Figure 7 illustrates Bode diagrams for the transfer functions from the converter switching period to the converter output voltage, obtained in the nominal operating point conditions (400 V input voltage, 18 A output current), compared to the one from a single module (6 A output current).

Thus, we can conclude that the analytical approach used for a single LLC resonant converter module can be extended also to the three-phase interleaved solution. The generalized state-space averaging method for a single module, indeed, adequately predicts also the small-signal transfer function of the three-phase LLC converter with star connection.

A closed loop voltage control has been implemented for the three-phase LLC converter with transformer primary windings star connection, based on a digital PID controller implemented through a DSP by Texas Instruments. Figure 8 depicts the small-signal transfer function Bode diagrams of the interleaved converter including also the pre-conditioning circuitry. The PID controller analog function is also depicted together with the loop gain transfer function –T(s)–. The design for the PID controller was performed at 400V input voltage and maximum output current in order to obtain a loop bandwidth of approximately 5 kHz and a phase margin higher than 50 degrees. The digital implementation of the PID controller initially used Tustin bilinear transformation to maintain the system stability. Some tests have been performed at simulation level to initially check the LLC converter performances and finally some load-step variations have been measured on the prototype. Figure 9 depicts the measurements results of a load step variation from 0.2 A to 18 A on prototype of three-phase LLC converter with star connection. The system appears well-dumped, with a down-shoot of 620 mV and a fast recovery time of approximately 1.2 ms.

Figure 10 depicts, on the contrary, a load step measurement from 18 A to 0.2 A. The system exhibits a small over-shoot and a reasonable step response time. The recovery-time is however really long being the system after load-step at very low current absorption.

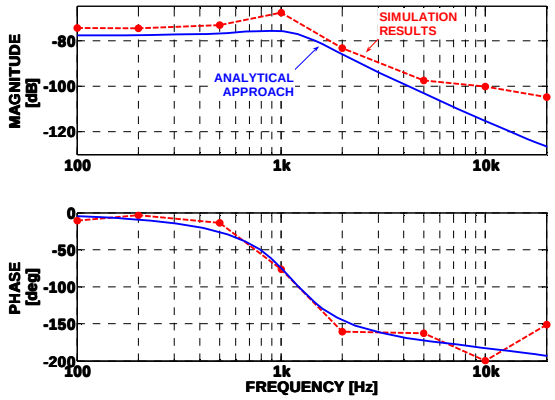

Fig. 6. Bode diagram for the small-signal transfer function ($\delta V_{OUT}/\delta F_{SW}$) of one module obtained through generalized state-space averaging method and through Simulink simulations. (V_{IN} = 400 V, I_{OUT} = 6 A)

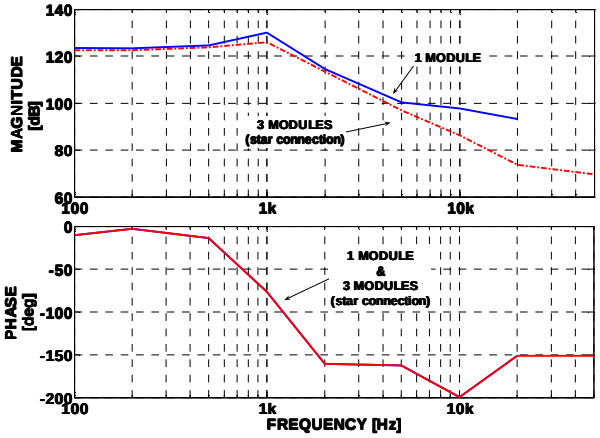

Fig. 7. Bode diagram for the small-signal transfer function ($\delta V_{OUT}/\delta T_S$) of one module compared to three modules with star connection. (V_{IN} = 400 V, I_{OUT} = 6 A for 1 module and I_{OUT} = 18 A for 3 modules)

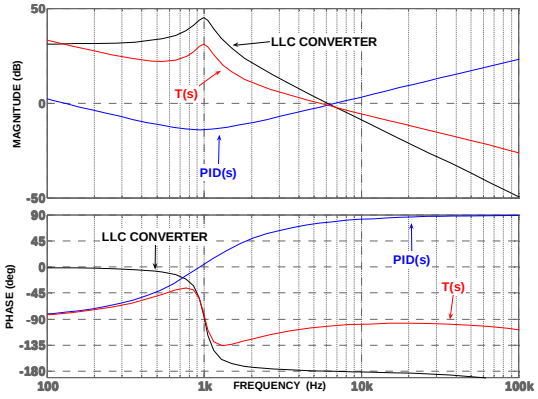

Fig. 8. Bode diagrams for:single module transfer function (including control pre-conditioning circuitry), PID regulator and system loop gain T(s). (V_{IN} = 400 V, I_{OUT} = 18 A)

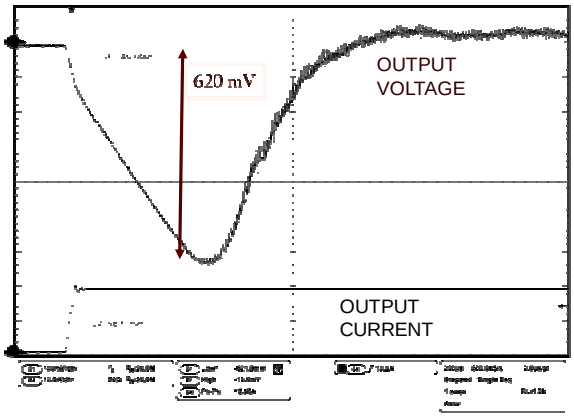

Fig. 9. Measurement on three modules with star connection for a load step from 0.2 A to 18 A. Ch1: converter output voltage (100 mV/div); Ch4: output current (10 A/div); time scale: 200 µs/div.

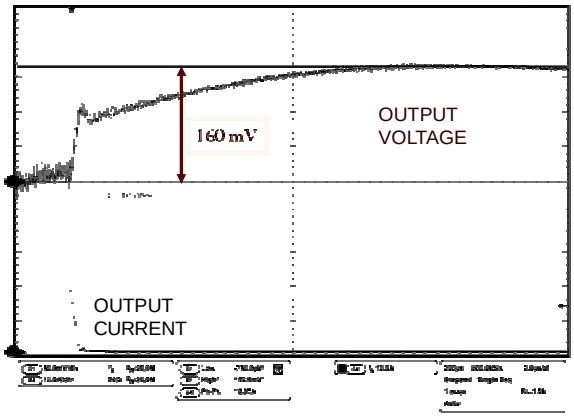

Fig. 10. Measurement on three modules with star connection for a load step from 18 A to 0.2 A. Ch1: converter output voltage (50 mV/div); Ch4: output current (10 A/div); time scale: 200 µs/div.

IV. PHASE-SHEDDING

The use of a three-phase LLC resonant converter with star connection allows to drastically reduce the output current ripple and consequently to minimize the filter capacitor. It is moreover mandatory to ensure the highest converter efficiency. The use of an increasing number of modules parallel connected allows to improve the efficiency for high output currents and, as for interleaved VRMs, suggests the possibility to opportunely shut down some phases in order to reduce power losses for low current absorption. The use of a star connection, instead of a simple parallel connection between modules, allows to introduce an inherent compensation of resonant component mismatch, while the traditional phase shedding is precluded. It is no more possible to simply turn off one or even two modules because of the floating star connection. For this reason it is necessary to adequately change the topology and modulation of the 3 phase LLC converter while performing phase-shedding in order to ensure a correct connection to ground of the resonant current.

Figure 11 depicts a possible "two-phase" solution obtained from the three-phase LLC with star connection by turning off module three (both M_{UP3} and M_{DN3} are turned off) and changing the driving signal phase-shift of module two from 120 degrees to 180 degrees (respect to module 1). In particular, module one and module two inverters are used as in full-bridge converters, sharing the series of resonant components for modules one and two.

Figure 12 depicts a possible "one-phase" solution for phase-shedding of the three-phase LLC converter with transformer primary windings star connection. In order to provide a return path for the resonant current flowing in module one, the lower MOSFET of the second half-bridge inverter (M_{DN2}) is kept on while M_{UP2}, M_{UP3} and M_{DN3} are turned off. The resonant components of the first and second phases are therefore put in series and operated as in a half-bridge solution by the module one inverter. The "one-phase" solution is not really based on the use of a single module, since while the half-bridge inverters for modules two and three are not switching, the resonant components of module two and its secondary-side rectifier are involved in the current conduction.

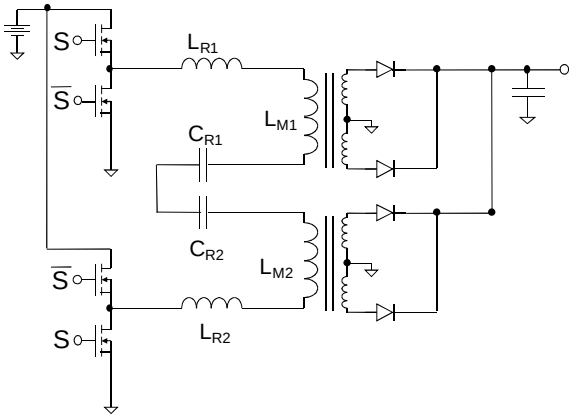

Fig. 11. Simplified scheme of the "two-phase" full-bridge topology for phase-shedding.

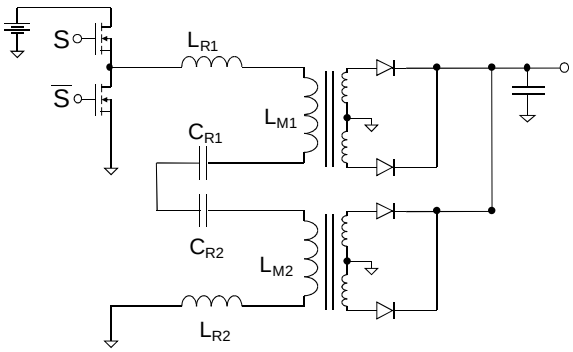

Fig. 12. Simplified scheme for the "one-phase" topology.

A. Converter Efficiency

Using the phase-shedding solution discussed above, a set of efficiency measurements was performed on the 3-phase LLC prototype with star connection. The results of such analyses are depicted in Figure 13. The measurements are initially performed on the three-phase LLC with all modules active. The output current is varied from 18 A (full load) to 1.8 A (10 % of the maximum power). A second series of the measurements is then performed in the full-bridge "two-phase" solution varying the output current from 12 A, that represents the maximum output power for two modules, to 1.2 A. It can be noticed that at 45 % of the maximum power (respect to the three-phase LLC converter) the two-phase solution equals the efficiency of the three-phase topology, suggesting the better condition to activate phase-shedding. Finally, the third efficiency measurements are performed on the "one-phase" solution for output current from 6 A to 0.6A. Also in this case an optimal condition can be found to switch from "two-phase" to "one-phase" (25 % of the maximum power).

The implementation of phase-shedding allows to improve the converter efficiency over a wide output current range. However, the necessary topology and modulation strategy modifications, compared to the initial three-phase interleaved solution, have two major drawbacks, that are analyzed hereafter.

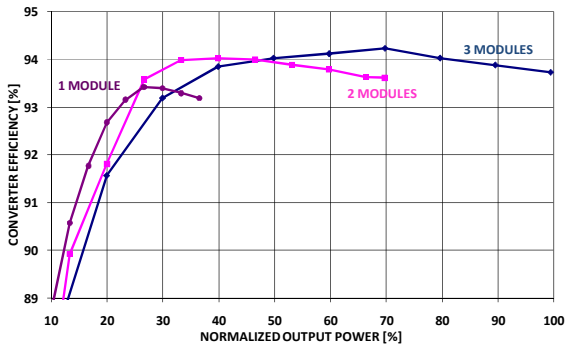

Fig. 13. Measured efficiency curves (@ V_{IN} = 400 V) as a function of the normalized output power (100% for I_{OUT} = 18 A): interleaved three-phase; "two-phase" full bridge and "one phase".

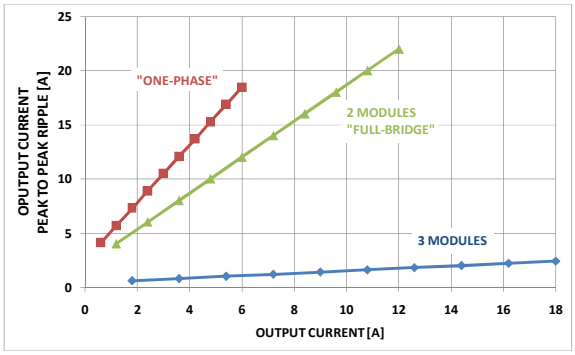

Fig. 14. Simulated peak to peak current injected on output filter capacitor as a function of output current (@ V_{IN} = 400V): interleaved three-phase; "two-phase" full bridge and "one-phase".

B. Effect on current ripple

The first drawback of phase-shedding is related to the output current ripple applied to the capacitive filter. While the interleaved solution allows to greatly reduce the output current ripple, both the full-bridge "two-phase" and half-bridge "one-phase" solutions exhibit a large output current ripple because a rectified sine wave current is applied to the capacitive filter. While for low output current this is not really a problem because also the peak to peak ripple decrease, for medium currents a trade-off between efficiency improvement and output current ripple is mandatory. Figure 14 shows the comparison of the total peak to peak current ripple injected into the output filter capacitor in the three phase-shedding conditions. It is evident that the benefits of the interleaved topology are lost when shutting-down one or two phases, with a large increase of total ripple. In the case of a phase-shedding implementation that maximize the converter efficiency, the output filter capacitor must be sized in the worst peak to peak ripple condition. In the case under test, C_{OUT} must be designed to adequately filter 15 A peak to peak (maximum ripple current if "one-phase" condition is turned-on at 25 % output power level and "two-phase" topology is activated at 45 % output power level).

C. Effect on Switching Frequency

The second drawback introduced by phase-shedding and topology modifications is related to the switching frequency range.

In order to correctly investigate such effect, let's initially introduce the power-supply voltage conversion ratio for a classical LLC resonant converter based on a unique module, as the one depicted in Figure 1 [6]. This converter can be conveniently described using the First Harmonic Approximation (FHA) technique which enables the analysis of resonant converters by means of classical complex ac circuit analysis. Figure 15 depicts the FHA equivalent circuit of the single module LLC converter focusing, in particular, to the ac resonant tank.

The resonant devices are expressed as:

$$C_R^* = C_R \qquad L_R^* = L_R \qquad L_M^* = L_M\,, \tag{2}$$

while the ac-equivalent load resistance in the FHA circuit can be evaluated as:

$$R_{EQ}^* = \frac{8}{\pi^2}\frac{V_{OUT}}{I_{OUT}}\,. \tag{3}$$

Finally, the FHA RMS values of input and output voltages for the ac resonant tank can be generally expressed as:

$$V_{O-FHA} = \frac{2\sqrt{2}}{\pi}V_{OUT} \tag{4}$$

$$V_{IN-FHA} = \begin{cases} \dfrac{\sqrt{2}}{\pi}V_{IN} & -HB- \\ \dfrac{2\sqrt{2}}{\pi}V_{IN} & -FB- \end{cases} \tag{5}$$

In particular, it must be noticed the doubled RMS input voltage applied to the resonant tank by means of the full-bridge switching topology (exploited in the "two-phase" solution for phase-shedding).

The normalized LLC voltage conversion ratio, also known as "voltage gain" can be therefore evaluated as:

$$M_{FHA} = \frac{n \cdot V_{O-FHA}}{V_{IN-FHA}} = \left\| \frac{sL_M^* \,//\, n^2 R_{EQ}^*}{\frac{1}{sC_R^*} + sL_R^* + \left(sL_M^* \,//\, n^2 R_{EQ}^*\right)} \right\| = \frac{1}{\sqrt{\left(1 + \frac{L_R^*}{L_M^*} - \frac{L_R^*}{L_M^*}\frac{f_R^2}{f_{SW}^2}\right)^2 + Q^{*2}\left(\frac{f_{SW}}{f_R} - \frac{f_R}{f_{SW}}\right)^2}} \quad (6)$$

where:

$$f_R = \frac{1}{2\pi\sqrt{L_R^* C_R^*}} \quad (7)$$

and

$$Q^* = \frac{1}{n^2 R_{EQ}^*}\sqrt{\frac{L_R^*}{C_R^*}} \cdot \quad (8)$$

The general expression for the dc voltage conversion ratio can also be evaluated using (4), (5) and (6):

$$M_{LLC} = \frac{V_{OUT}}{V_{IN}} = \begin{cases} \frac{1}{2n} M_{FHA} & -HB- \\ \frac{1}{n} M_{FHA} & -FB- \end{cases} \quad (9)$$

The analysis above can now be applied to the three-phase interleaved LLC resonant converter in the three different topologies created by phase-shedding.

The voltage conversion ratio of the interleaved three-phase topology (that is all three modules activated) is equivalent to that of a single module delivering 1/3 of the total current. Thus, the interleaved three-phase dc voltage conversion ratio can be evaluated as:

$$M_{LLC-3} = \frac{1}{2n} M_{FHA}\left(Q^* = Q_{LLC-3}\right), \quad (10)$$

with

$$Q_{LLC-3} = \frac{1}{n^2 3\frac{8}{\pi^2}\frac{V_{OUT}}{I_{OUT}}}\sqrt{\frac{L_R}{C_R}} \quad (11)$$

under the assumption that R_0 represents the total converter load resistance.

On the contrary, some additional topology manipulations must be introduced for the two remaining phase-shedding solutions. Fig. (a) depicts the FHA equivalent circuit of the ac resonant tank for the "two-phase" full bridge and "one-phase" topologies. In order to apply the converter "voltage gain" formula derived in (9) for a single module an adequate equivalent circuit can be obtained as depicted in Figure 16 (b) taking into account the effect of transformers turns ratio: series connection at primary side and parallel connection at secondary side. It must be noticed that the equivalent single module circuit exhibits a voltage drop at the series transformer primary side that is doubled compared to the circuit depicted in Figure 15. As a consequence, the "ac" voltage gain must be conveniently halved.

The resonance frequency for the "two-phases" and "one-phase" topologies appears to be the same as for the single module and the three-phase converter since $L_R^* = 2L_R$ and $C_R^* = C_R/2$. Equally, it must be noticed that the ratio L_R^*/L_M^* is unaltered for this topology modification, while the converter quality factor is modified by the variations of the characteristic impedance of the resonant circuit and R_{EQ}^*.

The dc voltage conversion ratio for the "two-phases" full bridge solution can be therefore evaluated as:

$$M_{LLC-2} = \frac{1}{n}\frac{M_{FHA}\left(Q^* = Q_{LLC-2}\right)}{2}, \quad (12)$$

where:

$$Q_{LLC-2} = \frac{1}{n^2 4 \cdot \frac{8}{\pi^2}\frac{V_{OUT}}{I_{OUT}}} 2\sqrt{\frac{L_R}{C_R}} \cdot \quad (13)$$

Finally, the dc voltage conversion ratio for the "one-phase" solution can be evaluated as:

$$M_{LLC-1} = \frac{1}{2n}\frac{M_{FHA}\left(Q^* = Q_{LLC-1}\right)}{2}, \quad (14)$$

with

$$Q_{LLC-1} = \frac{1}{n^2 4 \cdot \frac{8}{\pi^2}\frac{V_{OUT}}{I_{OUT}}} 2\sqrt{\frac{L_R}{C_R}} \quad (15)$$

Using (10), (12) and (14), the dc voltage conversion ratio as a function of the switching frequency can be calculated in all phase-shedding solutions evaluating therefore the corresponding switching frequency ranges. Figure 17 shows these dc voltage gains superimposed to the maximum and minimum thresholds corresponding to minimum input voltage and maximum one (converter specification listed in Table 1). In order to adequately compare the three topologies the dc voltage conversion ratios are evaluated at no-load and at "relative full load" that is the maximum deliverable current for each solution (I_{MAX} for the interleaved three-phase, 2/3 I_{MAX} for the "two-phases" and 1/3 for the "one-phase"). From the results plotted in Figure 17, as well from (10) and (12), it must be noticed that the interleaved three-phase and the "two-phase" full bridge solutions share the same switching frequency range between 63 and 96 kHz (note that $Q_{LLC-2}(2/3\ I_{MAX}) = Q_{LLC-3}(I_{MAX})$). On the contrary, the switching frequency range for the "one-phase" phase-shedding topology appears to be greatly reduced from 47 kHz to 53 kHz ($Q_{LLC-1}(1/3\ I_{MAX}) = 0.5Q_{LLC-3}(I_{MAX})$ while $M_{LLC-1}=0.5M_{LLC-3}$). Therefore particular attention must be put in the controller design, since the switching frequency reduction increases the resonant current amplitude. In particular, being the current sensing for the phase-shedding control implemented at primary side, an adequate hysteresis must be added to the comparator current thresholds, used to choose the appropriate number of modules to be activated, in order to avoid jittering.

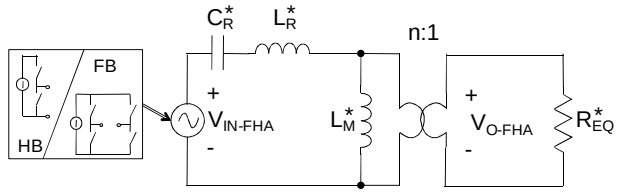

Fig. 15. First Harmonic Approximation circuit for a single module.

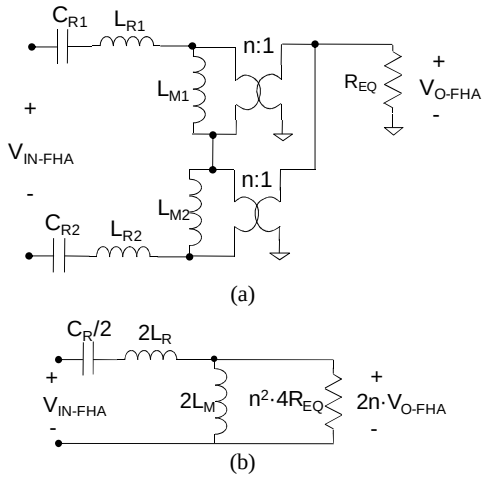

Fig. 16. First Harmonic Approximation equivalent circuit for ac resonant tank of the "two-phase" full-bridge and "one-phase" phase-shedding solutions. (a) represents the FHA of the circuit; (b) is the equivalent FHA single module topology.

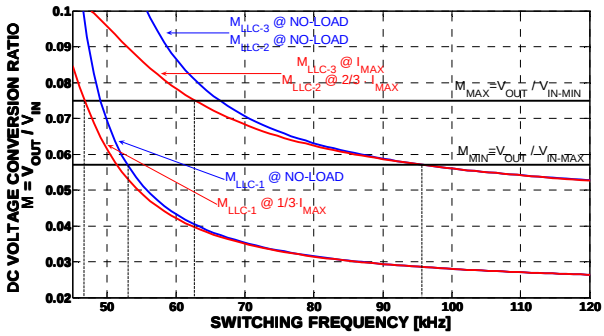

Fig. 17. DC voltage gain dependence from switching frequency for the interleaved three-phase LLC resonant converter in all three phase-shedding topologies. The minimum and maximum voltage gains to account for input voltage variations are also shown.

V. CONCLUSION

In this paper a three-phase interleaved LLC resonant converter topology is described and analyzed. The proposed topology is made by three half-bridge LLC converters with transformer primary windings star connection. This solution allows to drastically reduce the output current ripple compared to a single module, and exhibits an intrinsic balancing capability that is not common to other resonant interleaved solutions. Small-signal analysis of the proposed converter has been performed and a suitable digital control implemented. The possibility of turning off one or two phases depending on the overall output current level, is investigated, and the trade off between converter efficiency and output capacitor current ripple is discussed. Experimental results have confirmed the theoretical expectations.

REFERENCES

[1] *B. Yang*: "Topology investigation for front end dc/dc power conversion for distributed power system", Dissertation Virginia Polytechnic Institute and State University, 2003.

[2] *B. Yang, F. C. Lee, A. J. Zhang and G. Huang*: "LLC resonant converter for front end dc/dc conversion", IEEE APEC 2002, Vol.2, pp. 1108 – 1112.

[3] *T. Jin and K.. Smedley*: "Multiphase LLC series resonant converter for microprocessor voltage regulation", IEEE 41st Industry Applications Conference – IAS, Vol. 5, 8-12 Oct. 2006, pp. 2136 – 2143.

[4] *I. Apeland and R. Myhre*: "Phase-shifted resonant converter having reduced output ripple", US patent 6970366 B2, Nov. 2005.

[5] *H. Figge, T. Grote, N. Froehleke. J. Boecker and P. Ide*: "Paralleling of LLC resonant converter using frequency controlled current balancing", IEEE PESC 2008, June 2008 pp. 1080 – 1085.

[6] *ST Microelectronics AN 2450*: "LLC resonant half-bridge converter design guideline", Mar. 2007.

[7] *ST Microelectronics AN 2393*: Reference design: wide range 200W L6599-based HB LLC resonant converter for LCD TV & flat panels, Aug. 2006.

[8] *C. Adragna, S. De Simone and C. Spini*: "A design methodology for LLC resonant converters based on inspection of resonant tank currents", IEEE APEC 2008, 24-28 Feb. 2008, pp.1361 – 1367.

[9] R. Sanders, J. M. Noworolski, X. Z. Liu, G. Verghese, "Generalized Averaging Method for Power Conversion Circuits," IEEE Trans. On Power Electronics, Vol.6, No.2, April 1991, pp.251-258.